Diamond and Related Materials, 2 (1993) 1012–1019

Diamond radiation detectors

D. R. Kania, M. I. Landstrass and M. A. Plano
Crystallume, 125 Constitution Dr., Menlo Park, CA 94025 (USA)

L. S. Pan and S. Han
Lawrence Livermore National Laboratory, Livermore, CA 94550 (USA)

Abstract

Diamond radiation detectors have a lengthy history. Photoconductive UV detectors were developed in the 1920s and ionizing radiation detectors were created in the 1940s. However, these devices encountered restricted usage owing to the limitations of natural diamonds. Specifically, these limitations were the small size and lack of control of the material characteristics. Recent advances in the high quality growth of diamond by chemical vapor deposition have created the opportunity for the application of this material in practical detectors.

1. Introduction

Diamond is a very interesting material with many exotic properties. The large band gap, radiation hardness, optical transparency, large saturated carrier velocities and low atomic number of diamond all make it a very attractive candidate for applications in radiation detection. In this paper we will confine the discussion to radiation detectors in the form of two-terminal electronic devices with a metal–insulator–metal (MIM) structure. The insulator is undoped, intrinsic diamond and the metals nominally form ohmic contacts; no p- or n-type junctions are required. In standard semiconductor materials such as silicon the thermally generated leakage currents preclude the operation of detectors in this type of structure. Leakage currents are suppressed by the use of reverse-biased junctions. In this paper we will be discussing the simplest of diamond devices.

Any radiation that generates free carriers in the diamond can be detected. These radiations include electromagnetic radiation with an energy of greater than 5.5 eV. This incorporates UV, X-rays and γ rays. High energy particle radiation such as α particles, electrons, neutrons, pions and other exotic particles can also be detected. The fundamental mechanism of detection is independent of the exciting radiation, *i.e.* the motion of free charges in an applied electric field across the device. These free charges, electrons and holes, are created by the interaction of the radiation with the diamond. An excellent review of the basic physics of the relevant interactions of radiation and matter can be found in ref. 1.

2. Radiation detection

A schematic diagram of an MIM diamond detector is shown in Fig. 1. A high resistivity diamond is sandwiched between two metal electrodes. An external voltage provides an electric field across the device. Mobile charges produced by absorbed radiation drift in this electric field and generate a current in the external circuit. Detectors can be operated in one of two modes: (1) pulse-counting mode or (2) current mode. Pulse counting refers to detection of individual quanta. The output signal may (spectroscopy) or may not (counting) be related to the energy of the particle. When a detector produces a current proportional to the intensity of a radiation field, it is operating in current mode. If the radiation field is pulsed, it is desired that the current pulse mimic the temporal evolution of the radiation burst. In this paper we will discuss the

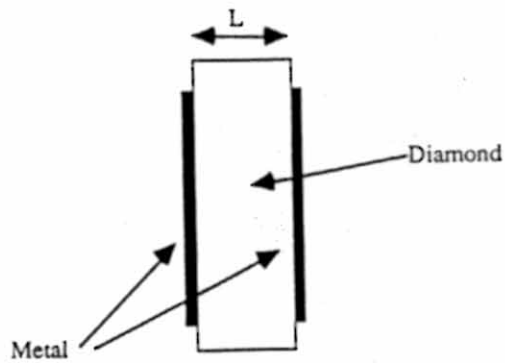

Fig. 1. Schematic diagram of a metal–insulator–metal detector. The electric field is applied across the two metal contacts.

0925-9635/93/$6.00

application of diamond detectors to pulse-counting and current mode detection of a wide variety of radiations.

For the present applications, all the radiation sensors we discuss rely on the generation of a current in an external circuit due to the motion of radiation-generated mobile charges in the diamond. The motion is driven by an externally applied electric field. The basic physics can be illustrated by assuming a uniform device with one mobile charge carrier that is generated by the radiation field. The mobile charges are generated at the rate $g(t)$. The generation rate is proportional to the intensity of the absorbed radiation divided by the average energy to form a mobile electron–hole (e–h) pair, ε. A rough estimate for ε is three times the band gap energy of the absorbing material for particles with an energy much greater than the band gap. The number of charges, $n(t)$, is related to the generation rate by

$$\frac{dn}{dt} = g(t) - \frac{n}{\tau}$$

where τ is the lifetime of the mobile charges in the device. The lifetime may be limited by material defects or device geometry. For an impulsive excitation,

$$n(t) = n_0 \exp\left(-\frac{t}{\tau}\right)$$

$$n_0 \approx gT$$

where n_0 is the density of mobile charges at $t=0$ and T is the pulse width. For a continuous excitation,

$$n = \tau g$$

The current density is

$$j(t) = nev$$

$$v = \mu(E)E$$

where ne is the total mobile charge, v is the carrier velocity, E is the applied electric field and $\mu(E)$ is the field-dependent mobility. The charge collection or transit time is $\tau_c = L/v$. For a single particle of energy E_p the charge generated in the external circuit, q, is

$$q = \frac{Qv\tau}{L} = \frac{Qd}{L} \tag{1}$$

where Q is the total mobile charge created by the particle, eE_p/ε. This implies $q/Q = d/L$, where d is the average distance a charge carrier moves. If $d > L$ and there are nominal boundary conditions, all the charge will be collected. If $d < L$, only a fraction will be collected. In the case of incomplete charge collection, care must be taken in the design of the device to eliminate the effects of space charge build-up. The uncollected charge in the device can result in the accumulation of a net charge within the device. Even if uniformly distributed, this will result in a distortion of the electric field distribution within the device. This typically manifests itself in reduced charge collection efficiency. From this analysis we can see that the important material parameters are μ and τ or their product, $d = \mu E\tau$. The above analysis is extremely simplified and can be found in greater detail, albeit from a different perspective, in ref. 1 for ionizing radiation detection and in ref. 2, from a photoconductivity radiation-modulated resistor point of view. A first-principles analysis based on Gauss' law can be found in early papers by Ramo [3] and Shockley [4].

3. Properties of diamond

Although silicon, the most common detector material, will not be replaced by diamond, diamond does possess many inherent advantages for specific applications in radiation detection. Table 1 summarizes some of the important properties of diamond and silicon.

As previously mentioned, the high resistivity of intrinsic diamond eliminates the need for reverse-biased p- or n-type junctions to suppress thermally generated currents. The leakage currents and their fluctuations are an undesirable noise source in radiation measurements and can limit the magnitude of the applied electric field. These effects dramatically impact device performance. In addition, the low dielectric constant reduces the capacitance of a diamond device, a distinct advantage in most detector applications. Thus a diamond radiation detector is a simple two-terminal metal–insulator–metal device with an inherently low leakage current. The large band gap of diamond significantly reduces the sensitivity to visible radiation, thus allowing windowless operation in many applications. This property also permits the operation of detectors at high

TABLE 1. Properties of diamond and silicon

Property	Diamond	Silicon
Density (g m^{-3})	3.5	2.32
Band gap (eV)	5.5	1.1
Resistivity (Ω cm)	$>10^{12}$	10^5
Breakdown voltage (V cm^{-1})	10^7	10^3 (pn junction)
Electron mobility (cm^3 V^{-1} s^{-1})	1800	1500
Hole mobility (cm^3 V^{-1} s^{-1})	1200	500
Saturation velocity (μm ns^{-1})	220	100
Dielectric constant	5.6	11.7
Neutron transmutation cross-section (mb)	3.2	80
Energy per e–h pair (eV)	13	3.6
Atomic number	6	14
Av. min. ionizing signal per 100 μm (e)	3600	8000

temperatures while maintaining a low noise. Diamond is also radiation hard and chemically inert. This lends it to applications in harsh environments where silicon detectors could not operate. The significantly smaller neutron transmutation cross-section is one manifestation of the radiation hardness of diamond. Experiments have demonstrated diamond's superior radiation hardness against neutron [5] and electron [6] irradiation.

The high saturated carrier velocity permits the high speed and high count rate operation of diamond detectors. This characteristic is important in high event rate applications. It reduces the effects of pulse pile-up or the summation of multiple events into an apparent single event. The low atomic number of diamond is closely matched to soft human tissue. This is a critical property for radiation dosimetry applications. The absorption of ionizing radiation is a strong function of the atomic number. For example, for photons with an energy of less than 100 keV the absorption cross-section scales as Z^4. Therefore diamond detectors approach the ideal situation when the atomic number of the detector matches that of the tissue being measured, $Z_{tissue} \approx 7.5$. The chemical inertness of diamond is another important characteristic for medical applications.

Although the low atomic number of diamond is an advantage for dosimetry, it is a disadvantage for measuring penetrating radiation such as high energy X-rays or γ rays. The low Z implies a small cross-section and poor detection efficiency. At the same time the large band gap of diamond implies that the average energy to form an electron–hole pair is larger than in silicon, further reducing its sensitivity. The higher density of diamond is not large enough to compensate for this effect. As a result, the average minimum ionizing particle signal generated is over a factor of 2 smaller for diamond than for an equivalent thickness of silicon. In summary, diamond detectors have the advantage of being simple, visible-blind, radiation-hard and high speed devices. The sensitivity will be a strong function of the type of radiation to be detected, although for equivalent geometries diamond will be less sensitive than silicon.

4. History

The use of diamond as a radiation detector has its origins early in this century. Gudden and Pohl in 1923 used a photoconductive detector to study the absorption characteristics of diamond [7]. Robertson *et al.* used photoconductivity to establish the classification of type I and II diamonds [8]. Hofstadter reviewed the work on natural diamond in the 1949 issue of *Nucleonics* [9]. The goal of this early research was to produce solid state "crystal counters" to replace gas counters in support of nuclear physics research. Much of the research was oriented toward finding useful samples of diamond, so-called counting diamonds. For example, Friedman *et al.* [10] and Freeman and Van der Velden [11] showed that type IIa, low birefringence diamonds are best for radiation detectors.

More quantitative work followed. Kennedy [12] studied the pulse height spectrum of high energy electrons as a function of electric field strength in diamond. Champion and Wright [13] looked at α particles. The goal of this research was to determine the mean energy to produce an electron–hole pair for different radiations in diamond. McKay's [14] current mode work used 14 keV electrons to excite natural diamond detectors. This work also addressed the effects of internal space charge fields resulting from incomplete charge collection in the devices. Studies were continued by Dean and Male [15] to measure the detection efficiency of β and α particles. A sample pulse height spectrum is shown in Fig. 2. The detector was a natural IIa diamond, 14.5 μm thick, with 10 V bias. The α particle source was ^{241}Am, which emits an α particle at 5.5 MeV.

Konorova *et al.* [16] showed that carrier velocity saturation causes a saturation in the detector current at high electric fields and that nitrogen impurities affect the carrier lifetime in the sample. Later, Konorova and Kozlov [17] showed that space charge effects can be eliminated by providing an injecting contact. They also showed detailed conversion electron pulse height spectra. Kozlov, *et al.* [5] built space-charge-free devices, measured the rise time of α-irradiated diamond detectors and discussed the advantages and disadvantages of diamond detectors in specific applications. They pointed out that one distinct disadvantage of natural diamonds was the lack of control of the crystal characteristics. Using time-of-flight techniques, Canali *et al.* measured the high field drift characteristics of diamond, which demonstrated that the carrier velocity for electrons and holes exceeds 10^7 cm s^{-1} for $E > 2 \times 10^4$ V cm^{-1} [18].

Applications of diamond in X-ray and γ ray dosimetry were explored by several authors [19–23]. In this application the low Z of diamond is used to mimic the absorption characteristics of soft human tissue. The chemical inertness of diamond made it an ideal candidate for an *in vivo* sensor. Again, these researchers point out the lack of process control in natural diamond. In this research, synthetic diamonds were used to address this issue with some success, indicating that process control of the material is an important step forward [22].

Single-crystal diamond photoconductors have been used as UV and soft X-ray detectors. Early studies were focused on understanding impurities and defects in the diamonds [24]. Recently, diamond detectors have been used to measure the soft X-ray fluxes from intense sources of radiation such as plasma pinches [25] and

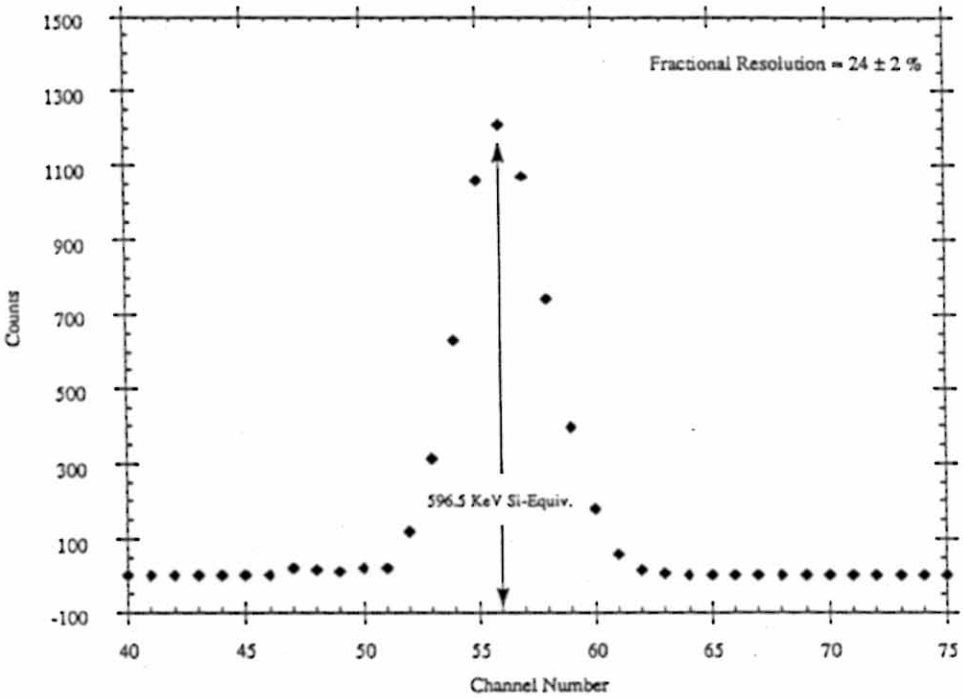

Fig. 2. α Particle spectrum from a type IIa natural diamond, 14.5 μm thick, biased at 10 V. The α particle source was ^{241}Am emitting at 5.5 MeV.

laser plasmas [26]. In these applications the optical blindness of the diamond is an important feature.

In general, the development of diamond radiation detectors was limited by the availability of reproducible samples, process control of the sample characteristics and limited size. Diamond grown by chemical vapor deposition (CVD) has the potential to address all these issues, resulting in unique and useful radiation detectors [27]. Recently, diamond radiation detectors have been fabricated from CVD diamond. These applications include UV sensors [28–30] and radiation-hard high energy particle detectors [31]. A more detailed discussion of applications of CVD diamond to radiation detectors will be presented in the following section.

5. CVD detector technology

Interest in radiation detectors has supplied some of the impetus for improving the detector properties of polycrystalline CVD diamond films. Over the past 5 years we have been involved in the characterization and fabrication of prototype diamond radiation sensors. The present discussion will be restricted to progress in polycrystalline films. The reader is referred to the paper by Landstrass *et al.* for a description of the state of the art in single-crystal homoepitaxial films [32] and to the paper by Pan *et al.* for more detail on polycrystalline films [33]. As a benchmark we use the characteristics of single-crystal IIa diamond. Such diamonds are known to contain a large density of defects and impurities, but they are readily available and have been successfully used in the past as radiation sensors.

As discussed earlier, an important figure of merit for radiation detectors is $d = \mu\tau E$. Two methods have been used to measure this property: (1) UV transient photoconductivity (PC) and (2) charge collection measurements using ionizing radiation. PC uses a large gap UV detector that is uniformly illuminated by a short intense burst of UV laser light. The resulting current pulse is recorded on a high speed oscilloscope (see Fig. 3). The decay of this pulse is related to the carrier lifetime τ and the amplitude and total charge are related to d (see eqn. (1)). This measurement is typically done on a lateral device, *i.e.*. the electric field direction and defining electrodes are on the growth surface. Only the top 2 μm of the device is sampled in these tests. A large variety of diamonds have been studied using this method by Pan *et al.* [28, 33].

The collection distance has also been measured using high energy electrons from a radiation source such as ^{90}Sr which emits 2.3 MeV β particles. This method employs the measurement of the total charge generated by a single high energy particle, q. The collection distance is determined from eqn. (1). In these vertical devices the electric field is parallel to the growth direction, typically extending from the substrate interface to the growth surface.

These techniques were applied to the measurement of the collection distance of CVD diamond samples. As

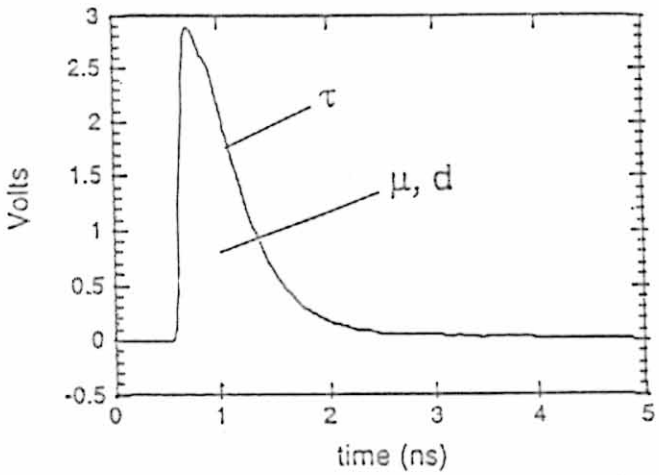

Fig. 3. Temporal evolution of a short pulse excitation of a diamond device. The device is excited with a 5 ps pulse of 200 nm light from a frequency-tripled dye laser. The decay of the pulse is related to the carrier lifetime, and the peak amplitude and area under the curve are related to μ and d.

the CVD diamond growth community matured, so did the detector quality of the material. Table 2 summarizes the evolution of the collection distance with time. The natural IIa single-crystal diamond was synthesized approximately 10^9 years ago and has a collection distance of between 20 and 50 μm at 10^4 V cm^{-1}. The earliest measurements on submicron thickness, d.c. plasma CVD samples were reported in 1989 by Pan *et al.* [34]. By modern standards these were poor quality films. The Raman spectrum indicated the presence of significant non-diamond-bonded carbon and the sample devices had a low resistivity. PC measurement showed $d = 10$ Å, indicating that the material was unsuitable for detectors.

In 1990 higher quality films approximately 5 μm thick produced by microwave CVD were tested. The non-diamond-bonded carbon component was reduced dramatically, the device resistivity was greater than 10^8 Ω cm and the collection distance was approaching 0.1 μm. Subsequent developments in diamond growth increased d to 2.5 μm in 1991 and 20 μm in 1992. The most recent work by Plano and Landstrass [35] has a measured mobility (sum of electrons and holes) equal to that of IIa single-crystal diamonds.

TABLE 2. Evolution of the properties of polycrystalline CVD diamond films

Date	d (μm) at 10^4 V cm^{-1}
~10^9 BC (natural IIa)	20–50
AD 1989	10^{-3}
AD 1990	10^{-1}
AD 1991	2.5
AD 1992	20

During this development, several correlations of the electronic properties with other material properties were noted. In general, the more characteristics of single-crystal diamond the material had, the better were the electrical properties. This was true of the UV absorption coefficient, sample resistivity and Raman spectrum. In the Raman spectrum both the width of the diamond peak and evidence of non-diamond bonding were important. It was also noted in this work that a gradient in d exists along the growth direction. The electrical quality of the diamond improved with film thickness. This is a direct analog of the results observed by Graebner *et al.* [36] in thermal conductivity measurements on a source of CVD samples grown to different thicknesses under identical conditions. Using PC, which probes the electrical properties of the surface, the collection distance at the growth surface as a function of the thickness was determined (see Fig. 4). This may indicate a reduction in the defect density of the material as it grows thicker.

The production of advanced polycrystalline CVD diamond has led to one near-term detector application: visible-blind, UV and soft X-ray detectors. The 1 mm gap test structures used in refs. 28, 33 and 34 are in fact such detectors; however, they are unfortunately extremely inefficient devices because $d/L \ll 1$. This is a result of $d \ll L$. A single small gap $d \approx L$ could have high efficiency but will have a very small active area. An efficient and large area detector can be constructed by using an interdigitated electrode structure as described in Fig. 5. More details on this structure are presented in ref. 29 and 32. These devices are appropriate for UV and soft X-ray detection because of the short penetration depth of this radiation, less than 10 μm from 5.5 eV to 2 keV (see Fig. 6). This results in all the mobile charges being produced near the surface of the

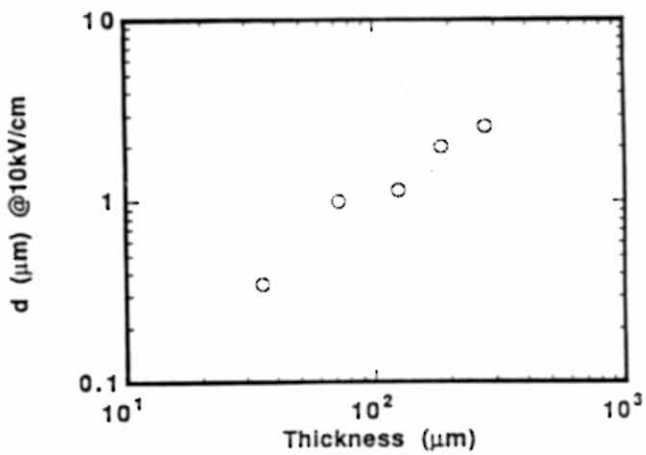

Fig. 4. Plot of carrier collection distance as a function of CVD diamond sample thickness. The samples were grown under identical conditions.

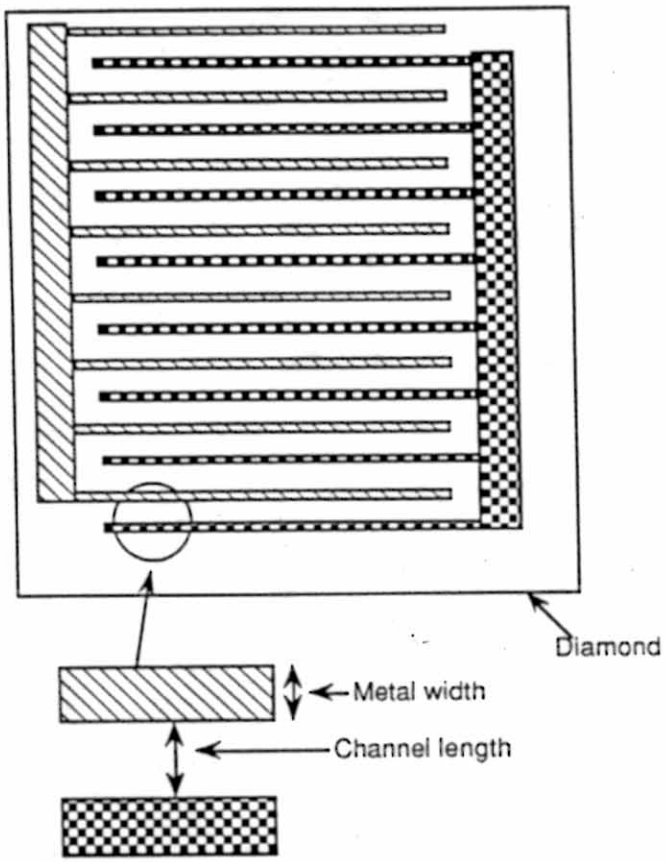

Fig. 5. Schematic diagram (top view) of a diamond UV radiation detector. Shown in the figure is an interdigitated electrode configuration for optimum collection efficiency.

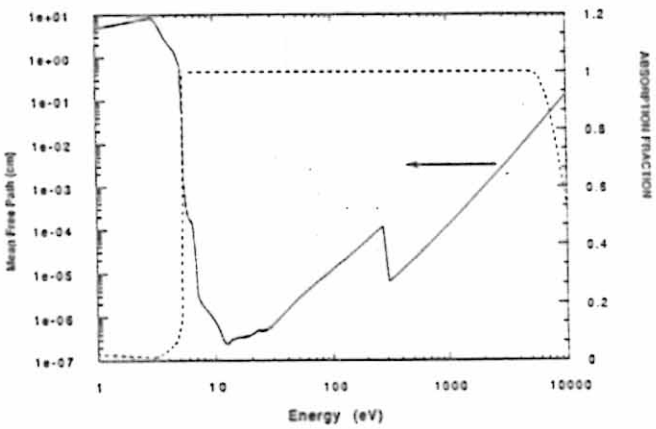

Fig. 6. Photon mean free path (——) in diamond as a function of photon energy, and absorption fraction (---) for a detector 1 mm thick.

device, resulting in efficient charge collection. In addition, there is no apparent *dead layer* in a diamond device. In silicon UV and soft X-ray detectors, great care must be taken to minimize the thickness and maintain the uniformity of the surface oxide. This oxide is a very strong UV and soft X-ray absorber. This absorbed radiation does not contribute to the detector signal, hence the name dead layer.

In high energy physics experiments the next-generation high energy, high luminosity hadron colliders, *e.g.* the Superconducting Super Collider (SSC) and the Large Hadron Collider (LHC), require detectors that can operate at high event rates and withstand severe radiation environments. The simplicity, high charge collection speed and radiation hardness of diamond radiation detectors have significant advantages over existing technology. A collaborative effort is under way to develop CVD diamond radiation detectors for this application, the DIAMAS collaboration [37].

The dimensions of the detector are dictated by two criteria: (1) charge collection time of about 1 ns and (2) charge generation (collection) of about 10^4 charges for a minimum ionizing particle, *e.g.* a high energy electron. The first criterion is dictated by the expected event rate in these experiments, 10^8 Hz. The second criterion is determined by the required signal level for charge-sensitive preamplifiers. Therefore an MIM detector element requires diamond with the following characteristics:

$L = 200\ \mu m$
$d = 200\ \mu m$
$\mu = 2000\ cm^2\ V^{-1}\ s^{-1}$
$E = 10^4\ V\ cm^{-1}$
$v = 2 \times 10^7\ cm\ s^{-1}$
$q = 7000\ e\ (MIP)$
$\tau = 1\ ns$

A diamond-based detector has been designed by the DIAMAS collaboration. The radiation hardness of the diamond permits a much more compact design than conventional (silicon) detectors do. These detectors are shaped like right circular cylinders. The length of a conventional SSC detector is 35 m with a radius of 12.5 m. DIAMAS is only 6 m long and 3.5 m in radius. This is a significant size and potential cost reduction while matching or exceeding the performance characteristics of the conventional technology.

As discussed in the last section, the current state of the art in diamond films is $d \approx 20\ \mu m$. Full implementation of diamond in a detector will require continued improvement in the material. Nevertheless, some important proof-of-principle experiments have been performed. These experiments demonstrated the detection of single minimum ionizing particles with CVD diamond detectors. These tests were performed at KEK in Japan and TRIUMF in Canada [31].

Electrons with an energy greater than 100 MeV were used. The detectors were simple vertical MIM structures, as depicted in Fig. 1, with $L = 250\ \mu m$. The charge collection efficiency of these devices was determined by comparison of the signal level with that of a reference silicon detector and by using first-principles calculations

of the energy deposited using the EGS Monte Carlo simulations. The two methods of analysis agree. For the samples tested, a charge collection distance of greater than 10 μm has been observed. Sample data are shown in Fig. 7. Rate-dependent studies were also performed. No degradation in pulse height was observed for rates of up to 10^4 particles cm^{-2} s^{-1}.

A large area (3×3 cm^2) prototype detector is being assembled. The active area of the device is divided into three independent channels of size 0.75×2.75 cm^2. This device will be used to study the uniformity of the detector and to gain experience in using large area diamond multichannel devices. Eventually, several layers will be stacked as a prototype tracking detector.

6. Conclusions

Diamond radiation detectors have a lengthy history. Photoconductive UV detectors were developed in the 1920s and ionizing radiation detectors were created in the 1940s. However, these devices encountered restricted usage owing to the limitations of natural diamonds. Specifically, these limitations were the small size and lack of control of the material characteristics. Recent advances in the high quality growth of CVD diamond have created the opportunity for the application of this material in practical detectors. The figure of merit for radiation detectors is the average distance a carrier moves. State-of-the-art polycrystalline films have equaled the performance of single-crystal IIa natural diamonds.

Applications of this material include UV detectors and large detectors for high energy physics experiments. As the quality of CVD diamond continues to improve, so will the range of applications of this unique material.

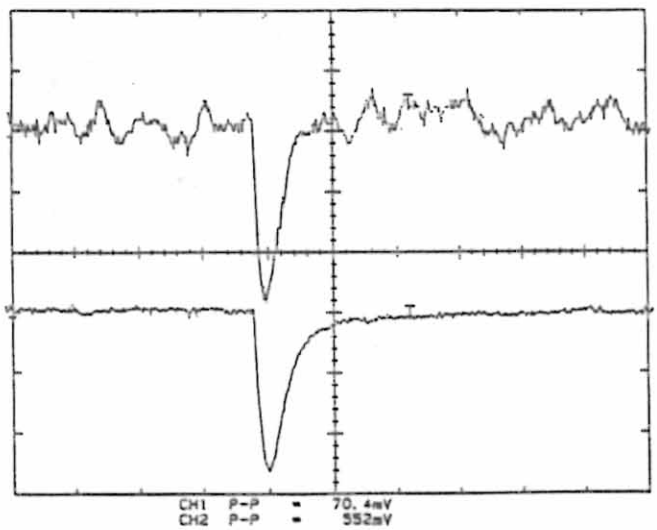

Fig. 7. Sample data demonstrating the detection of single high energy electrons (MIPs) in a CVD diamond detector. The lower trace is from a reference silicon detector and the upper trace is the CVD diamond pulse.

Acknowledgments

This work was supported by the Super Conducting Supercollider Laboratory, the Texas National Accelerator Laboratory and the Department of Energy at Lawrence Livermore National Laboratory under contract W-7405-Eng-48.

References

1 G. F. Knoll, *Radiation Detection and Measurement*, Wiley, New York, 1989.
2 R. H. Bube, *Photoconductivity of Solids*, Wiley, New York, 1960.
3 S. Ramo, *Proc. IRE, 27* (1939) 584.
4 W. Shockley, *J. Appl. Phys., 1* (1938) 636.
5 S. F. Kozlov, R. Stuck, M. Haga-Ali and P. Siffert, *IEEE Trans. Nucl. Sci. NS-22* (1977) 160.
6 M. Geis, MIT Lincoln Laboratory, personal communication, 1990.
7 B. Gudden and R. Pohl, *Z. Phys., 17* (1923) 331.
8 R. Robertson, J. J. Fox and A. E. Martin, *Philos. Trans. R. Soc. Lond. A, 232* (1934) 463.
9 R. Hofstadter, *Nucleonics, 4* (April 1949) 2.
10 H. Friedman, L. S. Birks and H. P. Ganvin, *Phys. Rev., 73* (1948) 186.
11 G. P. Freeman and H. A. Van der Velden, *Physics, 18* (1952) 1.
12 P. J. Kennedy, *Proc. R. Soc. A, 253* (1959) 37.
13 F. C. Champion and F. C. Wright, *Proc. Phys. Soc., 73* (1959) 385.
14 K. G. McKay, *Phys. Rev., 77* (1950) 816.
15 P. J. Dean and J. C. Male, *J. Phys. Chem. Solids, 25* (1964) 311.
16 E. A. Konorova, S. F. Kozlov and V. S. Vavilov, *Soc. Phys.—Solid State, 8* (1966) 1.
17 E. A. Konorova and S. F. Kozlov, *Soc. Phys.—Semi Cond., 4* (1971) 1600.
18 C. Canali, C. Jacobini, F. Nava, L. Reggiani and S. F. Kozlov, *Inst. Phys. Conf. Ser., 43* (1978) 327–330.
19 W. F. Cotty, *Nature, 177* (1956) 1075.
20 S. F. Kozlov, E. A. Konorova, Y. A. Kaznetsov, Y. A. Salikov, V. I. Rodko, V. R. Grinberg and M. L. Medman, *IEEE Trans. Nucl. Sci., NS-24* (1977) 235.
21 E. A. Burgermeister, *Phys. Med. Biol., 26* (1981) 265.
22 B. Planskey, *Phys. Med. Biol., 25* (1980) 519.
23 T. L. Nam, R. J. Keddy and R. C. Burns, *Med. Phys., 14* (1987) 596.
24 P. Denham, E. C. Lightowlers and P. J. Dean, *Phys. Rev., 161* (1967) 762.
25 R. B. Spielman, *Rev. Sci. Instrum., 63* (1992) 5056.
26 D. R. Kania, L. Pan, H. Kornblum, P. Bell, O. L. Landen and P. Pianetta, *Rev. Sci. Instrum., 2765* (1990) 816.
27 M. N. Yoder, Novel electron devices based on the unique properties of diamond, in *Applications of Diamond Films and Related Materials*, Elsevier, Amsterdam, 1991, pp. 287–293.
28 L. S. Pan, D. R. Kania, S. Han, J. W. Ager III, M. Landstrass, O. L. Landen and P. Pianetta, *Science, 255* (1992) 830.
29 R. S. Wagner, *Proc. 12th Int. Conf. on the Application of Accelerators in Research and Industry, Denton, TX, 1992.*
30 S. C. Binari, M. Marchywka and H. B. Dietrich, *Diamond Relat. Mater.*, in press.
31 M. Franklin, A. Fry, K. K. Gan, S. Han, H. Kagan, S. Kanda,

D. Kania, R. Kass, S. K. Kim, R. Malchow, F. Morrow, S. Olsen, W. F. Palmer, L. S. Pan, F. Sannes, S. Schnetzer, R. Stone, Y. Sugimoto, G. B. Thomson, C. White and S. Zhao, *Nucl. Instrum. Methods A, 315* (1992) 39.

32 M. I. Landstrass, M. A. Plano, M. A. Moreno, S. McWilliams, L. S. Pan, D. R. Kania and S. Han, *Diamond Relat. Mater., 2* (1993) 1033.

33 L. S. Pan, S. Han, D. R. Kania, M. A. Plano and M. L. Landstrass, *Diamond Relat. Mater., 2* (1993) 820.

34 L. S. Pan, P. Pianetta, D. R. Kania, O. L. Landen, K. R. Ravi and L. S. Plano, Carrier mobilities and lifetimes in PECVD and natural diamond photoconductors, *Proc. First Int. Symp. on Diamond and Diamond-like Films*. Electrochemical Society, Pennington, NJ, 1989, pp. 424–433.

35 M. A. Plano, M. I. Landstrass, S. McWilliams, L. S. Pan, S. Han, D. R. Kania and J. Ager, submitted to *Science*.

36 J. E. Graebner, S. Jin, G. W. Kammlott, J. A. Herb and C. F. Gardinier, *Appl. Phys. Lett., 60* (1992) 1576.

37 R. Plano, F. Sannes, S. Schnetzer, B. Stone, G. B. Thomson, K. K. Gan, T. Jensen, H. Kagan, R. Kass, F. Morrow, R. Malchow, T. Miller, S. Dregia, V. Subramaniam, D. Kania, S. Olsen, L. S. Pan, P. Pianetta and S. Prussin, Proposal to the SSC laboratory for subsystem R&D of diamond radiation detector, *SSC-EOI-9*, 1989.